Myosin Light Chain Kinase-regulated Endothelial Cell Contraction: The Relationship between Isometric Tension, Actin Polymerization, and Myosin Phosphorylation

Zoe M. Goeckeler* and Robert B. Wysolmerski*‡

Departments of *Pathology and ‡Anesthesiology, St. Louis University Health Science Center, St. Louis, Missouri 63104

Abstract. The phosphorylation of regulatory myosin light chains by the Ca^{2+}/calmodulin-dependent enzyme myosin light chain kinase (MLCK) has been shown to be essential and sufficient for initiation of endothelial cell retraction in saponin permeabilized monolayers (Wysolmerski, R. B., and D. Lagunoff. 1990. *Proc. Natl. Acad. Sci. USA.* 87:16–20). We now report the effects of thrombin stimulation on human umbilical vein endothelial cell (HUVE) actin, myosin II and the functional correlate of the activated actomyosin based contractile system, isometric tension development. Using a newly designed isometric tension apparatus, we recorded quantitative changes in isometric tension from paired monolayers. Thrombin stimulation results in a rapid sustained isometric contraction that increases 2- to 2.5-fold within 5 min and remains elevated for at least 60 min.

The phosphorylatable myosin light chains from HUVE were found to exist as two isoforms, differing in their molecular weights and isoelectric points. Resting isometric tension is associated with a basal phosphorylation of 0.54 mol PO_4/mol myosin light chain. After thrombin treatment, phosphorylation rapidly increases to 1.61 mol PO_4/mol myosin light chain within 60 s and remains elevated for the duration of the experiment. Myosin light chain phosphorylation precedes the development of isometric tension and maximal phosphorylation is maintained during the sustained phase of isometric contraction. Tryptic phosphopeptide maps from both control and thrombin-stimulated cultures resolve both monophosphorylated Ser-19 and diphosphorylated Ser-19/Thr-18 peptides indicative of MLCK activation.

Changes in the polymerization of actin and association of myosin II correlate temporally with the phosphorylation of myosin II and development of isometric tension. Activation results in a 57% increase in F-actin content within 90 s and 90% of the soluble myosin II associates with the reorganizing F-actin. Furthermore, the disposition of actin and myosin II undergoes striking reorganization. F-actin initially forms a fine network of filaments that fills the cytoplasm and then reorganizes into prominent stress fibers. Myosin II rapidly forms discrete aggregates associated with the actin network and by 2.5 min assumes a distinct periodic distribution along the stress fibers.

ENDOTHELIAL cells lining most vessels form a continuous layer that normally constrains proteins as well as formed blood elements to the vascular lumen. The loss of continuity of the endothelial sheet leads to increased permeability and the development of edema (30, 47, 51, 58, 71, 75). The increase in microvascular permeability by inflammatory and chemical mediators has been correlated with the presence of small gaps between adjacent endothelial cells. Furthermore, mediators that disrupt actin filaments and chelate extracellular calcium have been implicated in changes in macromolecular flux. The factors that may play a role in altering the barrier function of the endothelium leading to edema include: (*a*) loss of endothelial cell cohesion, (*b*) opening of tight junctions, (*c*) activation of intrinsic contractile activity, and (*d*) a disruption of the constitutive balance between homotypic cohesion, junctional integrity, and basal contractile forces. The possibility that active contraction opens intracellular junctions resulting in edema was originally proposed by Majno (51). Although several lines of evidence (41, 53, 60, 73) are now available to support this argument, the intracellular events regulating endothelial cell contractile activity remain to be elucidated.

The dynamic assembly, disassembly, and reorganization of the actin and myosin II cytoskeleton are believed to mediate a number of cellular contractile events in nonmuscle cells including endothelial cells. An understanding of the mechanism that regulates actin and myosin II cytoskeletal reorganization is fundamental to an understanding of endothelial cell contraction. We have used the phosphoryla-

Address all correspondence to Robert B. Wysolmerski, Dept. of Pathology, St. Louis University Health Science Center, 1402 South Grand Blvd., St. Louis, MO 63104.Tel.: (314) 577-8497. Fax: (314) 268-5132.

tion hypothesis for the regulation of smooth muscle contraction as a model for endothelial cell contraction (73, 74). The phosphorylation of myosin II regulatory light chains by myosin light chain kinase (MLCK)[1], a Ca^{2+}/calmodulin-dependent enzyme, is considered the essential requirement for activation both of smooth muscle (11, 19, 23, 24) and nonmuscle cell contraction (6, 29, 48). Studies in vivo and vitro have shown that phosphorylation of nonmuscle myosin II regulatory light chains by MLCK regulates the interaction of actin and myosin (2, 50), myosin II filament formation (12, 13, 27, 32), myosin ATPase activity (1, 31, 33), and in vitro motility (67). Phosphorylation of the regulatory light chain has also been shown to initiate cell retraction in permeabilized endothelial cells (73, 74) and fibroblasts (6, 29, 42).

We have previously shown that permeabilized endothelial cell preparations use a smooth muscle-like myosin based contractile system (73, 74). These preparations exhibited thiophosphorylation of myosin light chains that was concomitant with retraction, and both the thiophosphorylation and retraction were prevented by removal of MLCK and restored by replacement of purified MLCK together with Ca^{2+}/calmodulin.

To further pursue the mechanism for endothelial cell retraction, we developed a method to quantitatively measure isometric contraction in tissue culture. This system allows us to record rapid changes in basal and agonist stimulated tension over a period of hours to days. In this report, we present direct evidence in intact cells confirming the results from permeabilized preparations showing that MLCK-mediated phosphorylation of myosin regulatory light chains is tightly linked to initiation of endothelial cell retraction. Experiments have established a direct correlation between isometric tension, myosin light chain phosphorylation, actin polymerization, myosin II filament formation, and the spatial reorganization of the endothelial cytoskeleton.

Materials and Methods

Cell Culture

Human umbilical vein endothelial cells (HUVE) were harvested from human umbilical veins by the methods of Jaffe et al. (35). To eliminate contaminating fibroblasts or smooth muscle cells, primary HUVE isolates were seeded onto precast collagen gels prepared from a collagen/MCDB-107 solution composed of 4.0 ml bovine collagen (~3 mg/ml stock bovine calf skin collagen [Vitrogen Collagen Corp., Palo Alto, CA]), 4.4 ml 2 × MCDB-107, 1 ml FCS, 4 ml MCDB-107 containing 20% FCS, penicillin, streptomycin, and 0.4 ml 0.1 N NaOH. 15 ml of 1 mg/ml collagen/MCDB-107 was poured into a 100 × 20-mm Corning tissue culture dish and allowed to gel for 24 h at 37°C in a humidified incubator. Cells from six cords (average length 20 cm) were pooled and seeded onto the precast collagen gels in MCDB-107 medium supplemented with 20% FCS, 90 μg/ml heparin, 50 μg/ml endothelial cell growth supplement (ECGS; Collaborative Research, Inc., Waltham, MA), 5 μg/ml transferrin, 5 μg/ml insulin, 5 μg/ml penicillin, and 50 U/ml streptomycin. HUVE formed a confluent monolayer within 3–5 d and were maintained at confluence for an additional 5 d in which time contaminating fibroblasts and/or smooth muscle cells invade and migrate to the bottom of the collagen gel. Monolayers were subcultured by soaking gels in Mg^{2+} Ca^{2+}-free PBS containing 1 mM EGTA for 10 min followed by incubation with 10 ml of 0.05% collagenase (Type II; Worthington Biochemical Corp., Freehold, NJ) for 5 min at 37°C. Large sheets of HUVE, which detach from the underlying collagen gel within 2–5 min, were transferred to 50-ml conical centrifuge tubes containing equal volumes of 0.125% trypsin/EDTA for an additional 5-min incubation. After centrifugation, cells were seeded onto either fibronectin coated (3.3 μg/cm^2) 35 × 10-mm dishes for biochemical and morphological studies or directly onto precast collagen gels for tension measurements. Split ratios were determined such that cells were confluent when seeded. First passage HUVE monolayers 6 d after confluence were used throughout this study.

Experimental Procedure

24 h before experiments were performed, media was completely replaced with MCDB-107 containing 10% FCS and 5 μg/ml transferrin. Thrombin was prepared immediately before use at a concentration of 1 U/ml in MCDB-107 containing 5 μg/ml transferrin, 0.25% BSA and was maintained at 37°C. For most experiments unless otherwise noted, monolayers were briefly rinsed with MCDB-107 containing 0.25% BSA and then incubated with thrombin for the following time periods: 0, 30, 60, 90 s, 2.5, 5, 15, 30, and 60 min in a humidified 5% CO_2 atmosphere at 37°C. The monolayers were processed according to the individual protocols described below.

Isometric Tension Measurements

A newly designed tension apparatus that uses the same principles for HUVE isometric tension measurements as described previously (41) was used in the present study. The modified design allows us to perform simultaneous tension measurements on two monolayers and to prepare monolayers separate from the isometric tension apparatus. Fig. 1 *A* is a diagrammatic representation of the modified horizontal isometric tension monitoring apparatus (ITMA). The tension apparatus is constructed of a 24-gauge stainless steel base (24 × 28 cm) supported by three inch adjustable legs. 20-mm round support rods are secured to the base and connected at the apex (long edge) by 7-mm stainless steel rods. These rigid cross bars are used to suspend both the isometric force transducers and x, y, z multiaxis stage manipulators. Research grade isometric force transducers (model 52-9545; Harvard Apparatus Co., S. Natick, MA) are affixed to the crossbar by two rack and pinion stages (Harvard Apparatus Co., catalog no. 50-2617). Small adjustments can easily be made in the x, y direction with this configuration. Miniature x, y, z multiaxis stage manipulators (right and left handed; Stoelting Research Instruments, Wood Dale, IL) are attached to the opposite support column with 9.5-mm boss head clamps and two 20-cm stainless steel support rods. To prevent drifting of the x, y, z multiaxis stage manipulators over the duration of an experiment, the shafts of the micromanipulators are fitted with locking rings.

An advantage of the current design is the capability to prepare and grow monolayers unattached from the ITMA. Fig. 1 *B* is a schematic illustration of the removable specimen platform (RSP). This platform (125 × 130 cm) is designed to accommodate two 100-mm polymethylpenthene petri dishes. On either side of the petri dish attached to the base of the RSP are two brass support posts (4 cm × 2 mm). An alligator clip (no. 12, archer) soldered to the end of a brass shaft is attached to the support post by a 10-mm boss head clamp. The alligator clips are used to immobilize and maintain a fixed distance between the porous polyethylene holders thus reproducing the conditions under which monolayers are grown when attached to the ITMA (Fig. 1 *A*). This design prevents movement of the polyethylene holders as monolayers develop a stable basal tension. HUVE (3.5 × 10^6) were seeded onto the precast collagen gels (41) and maintained at 37°C in a humidified 5% CO_2 atmosphere. Monolayers were confluent within 3 d and used after stabilization of basal isometric tension (~5–7 d after confluence). Monolayers established on the RSP were maintained for 6 d at 37°C in a CO_2 incubator before being transferred to the ITMA.

Transducers were calibrated with a series of weights ranging from 10 to 500 dynes. To confirm that all of the recorded basal and stimulated tension was produced by the cells, the following calibrations were performed on all monolayers: (*a*) 3 μM cytochalasin D was added to abolish cellular tension and verify that tension was not attributed to the collagen matrix

1. *Abbreviations used in this paper*: ECGS, endothelial cell growth supplement; HUVE, human umbilical vein endothelial cells; ITMA, isometric tension monitoring apparatus; MLC, myosin light chain; MLCK, MLC kinase; RSP, removable specimen platform; SB, stabilization buffer; TLCK, *N*α-*p*-tosyl-L-lysine chloro-methyl ketone; TPCK, *N*-tosyl-L-phenylalanine chlormethyl ketone.

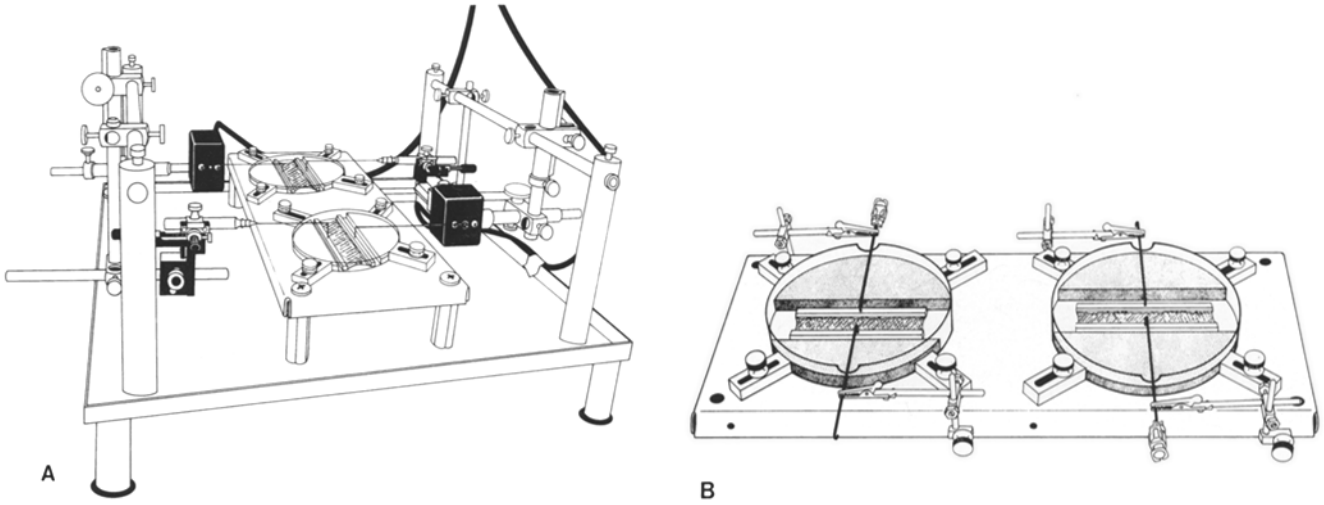

Figure 1. (*A*). Schematic representation of the horizontal ITMA. The ITMA has been designed to perform simultaneous measurements on paired monolayers and to prepare monolayers unattached from the apparatus. Both the force transducers and x, y, z, multistage micromanipulators are suspended from the rigid stainless steel cross supports by rack and pinion stages to facilitate attachment and alignment of the holders. Two polymethylpentene petri dishes are secured to a RSP. Porous polyethylene holders are positioned in the petri dishes within a 25-mm trough cut into the silicon elastomer. Collagen is cast between the polyethylene holders and allowed to polymerize for 24 h before seeding HUVE. (*B*). RSP allows monolayers to be prepared unattached from the ITMA. Platforms accommodate two polymethylene petri dishes. Porous polyethylene holders are placed within the petri dish and immobilized by alligator clips to prevent movement of the holders as the cells thin the collagen gel. Cell-populated collagen gels are cast identically to those prepared on the ITMA, maintained at 37°C for 6 d in a CO_2 incubator and transferred to the ITMA.

and polyethylene holders; (*b*) collagen gels were removed from the polyethylene holders and transducer output was recorded with the free floating holder (this procedure ensures that there is no downward deflection from the polyethylene holders contributing to recorded tension); and (*c*) polyethylene holders were removed and transducer output was recorded.

Tension was recorded using Modular Instruments Inc. (MI^2; Modular Instruments Inc., Malvein, PA) bioreport software package. For all measurements, MI^2 tissue bath data acquisition parameters were set as follows: (*a*) 2-s sample time, (*b*) frequency 32 hertz, and (*c*) sensitivity 0.3. Tension was recorded at 2-s intervals for the duration of all experiments.

Cell Labeling

For analysis of myosin phosphorylation, HUVE were labeled with either [^{35}S]methionine or [^{32}P]orthophosphoric acid or were double labeled with both. Because labeling monolayers in either methionine-free or phosphate-free media induces alterations in basal HUVE isometric tension and labeling in phosphate-free media for 2.5 h induces a 10–15 ± 5% increase in LDH release (45) above control cultures, the following labeling protocols were employed. To [^{35}S]methionine label cultures, HUVE were seeded at confluence in the presence of 25 μCi/ml [^{35}S]methionine in low methionine media (MCDB-107 containing 20 μM methionine, 20% methionine-free FCS, 75 μg/ml ECGS, and 90 μg/ml heparin), and maintained at confluence for 7 d. Monolayers were refed with low methionine media containing [^{35}S]methionine every 3 d. 24 h before an experiment, monolayers were washed twice with media and refed with low methionine MCDB-107 media supplemented with [^{35}S]methionine and 10% methionine-free FCS only.

To label with [^{32}P]orthophosphoric acid, cultures were washed twice with 2.5 ml of low phosphate media (MCDB-107 containing 20 μM sodium phosphate and 10% phosphate-free FCS) and then incubated with 2 ml of 75 μCi/ml [^{32}P]orthophosphoric acid in low phosphate media for 3 h at 37°C in a humidified 5% CO_2/95% air atmosphere. For double label experiments, cultures were first labeled with [^{35}S]methionine as stated above, washed twice with low phosphate media, and then incubated with [^{32}P]orthophosphoric acid as outlined above.

For experiments, [^{35}S]methionine-labeled cultures were washed with 2.5 ml MCDB-107 containing 0.25% BSA and then incubated with 1 U/ml thrombin in MCDB-107 supplemented with 0.25% BSA for the indicated times. Double labeled and [^{32}P]orthophosphoric acid-labeled cultures were washed in low phosphate MCDB-107 containing 0.25% BSA and then incubated in this medium containing 1 U/ml thrombin and 75 μCi/ml [^{32}P]orthophosphoric acid for the desired time intervals.

Immunoprecipitation of HUVE Myosin

HUVE myosin II was immunoprecipitated by a modification of our previously published methods (73). Experiments were terminated by aspirating media, flooding cultures with 600 μl of buffer A (25 mM Tris-HCl pH 7.9, 250 mM NaCl, 100 mM $Na_4P_2O_7$, 75 mM NaF, 5 mM EGTA, 5 mM EDTA, 1% NP-40, 0.5% DOC, 0.2 mM PMSF, 0.5 mM DTT, 100 μg/ml benzamidine, 100 μg/ml soybean trypsin inhibitor, 10 μg/ml of *N*-tosyl-L-phenylalanine chlormethyl ketone (TPCK), Nα-*p*-tosyl-L-lysine chloromethyl ketone (TLCK), aprotinin, leupeptin, pepstatin, and 15 mM mercaptoethanol at 4°C) and immediately placing them on a 4°C solid copper block. Monolayers were scraped up with a rubber policeman, culture dishes washed with an additional 100 μl of buffer A, samples combined and extracted on ice for 10 min. The total cell extract was centrifuged at 132,000 *g* for 10 min in a Beckman TL-100 ultracentrifuge. The supernatants were removed and incubated with 20 μl of a polyclonal rabbit anti platelet myosin II IgG fraction (15 mg/ml) (74) for 3 h at 4°C. Initial studies indicated that a variable degree of myosin II (ranging from 10 to 20% of total) remained associated with the 132,000-*g* pellet, so the cell pellets were extracted again by incubation in 200 μl of buffer A containing 600 mM NaCl, 50 mM KI, sonicated in a bath sonicator for two 5-s bursts and incubated on ice for 20 min. The insoluble material was sedimented at 132,000 *g*, extracts diluted with an equal volume of buffer A without NaCl or KI and then combined with the initial sample. After the 3-h incubation, prewashed protein A–Sepharose 4B was added for an additional hour. Immune complexes bound to protein A–Sepharose 4B were collected by centrifugation for 5 min at 12,000 *g* at 4°C. Pellets were first washed in 1 ml of buffer A then washed once with a 1:1 dilution of buffer A/PBS, twice with PBS, and finally once with a 1:1 dilution of PBS/distilled water. The pellets were dissolved in either 40 μl SDS sample buffer (44) or 100 μl of IEF sample buffer (28).

One- and Two-Dimensional Electrophoresis

One-dimensional SDS-PAGE was carried out in either 10% or 7.5–12% gradient vertical slab gels using the buffer system of Laemmli (44). Gels were stained with Coomassie blue, destained, dried at 70°C and exposed to Kodak X-OMAT x-ray film or phosphor screens.

Analysis of immunoprecipitated HUVE myosin II by two-dimensional gel electrophoresis followed the methods described by O'Farrell (55) as modified by Ludowyke et al. (48). For first dimensional separation of myosin light chains, IEF gels were prepared according to the procedure of Hochstrasser et al. (28).

Apparent pI values of the HUVE myosin light chains were determined by cutting tube gels into 5-mm pieces and soaking each gel piece in 1 ml of deionized, degassed water for 24 h. The pH of the solutions was measured using a Radiometer PHM 82 pH meter and the values plotted against distance from the top of the gel. The distances of migration of the myosin light chain isoforms/phosphorylation states from [^{35}S]-labeled cultures analyzed by two-dimensional electrophoresis were measured and pI values determined from the plot. The pI values were not corrected for the presence of urea (18).

Quantitative Analysis of HUVE Myosin Light Chain Phosphorylation

The stoichiometry of HUVE myosin light chain phosphorylation was determined by two-dimensional electrophoresis of [^{35}S]-labeled myosin light chains for direct estimates of the relative amounts of unphosphorylated, monophosphorylated, and diphosphorylated forms of myosin light chains present in control and thrombin treated monolayers. Scanned autoradiograms or phosphor plates were analyzed using Molecular Dynamics Image Quant Software and the state of myosin light chain phosphorylation calculated and expressed as either percentage of total myosin light chain phosphorylation or mol PO_4/mol MLC.

The mol/mol content was calculated from the following formula:

$$M/M = P_1 + 2(P_2)/U + P_1 + P_2 \quad (1)$$

where U = % unphosphorylated, P_1 = % monophosphorylated and P_2 = % diphosphorylated HUVE myosin light chains. The diphosphorylated myosin light chain (P_2) is multiplied by a factor of 2 to reflect the presence of two phosphate groups per light chain. The percentage of light chain phosphorylation was calculated by adding the densitometric values for each phosphorylation state for each isoform, i.e., unphosphorylated ($U_1 + U_2$), monophosphorylated ($M_1 + M_2$) and diphosphorylated ($D_1 + D_2$) (see Table II).

One-Dimensional Tryptic Peptide Mapping

[^{32}P]orthophosphoric acid-labeled immunoprecipitates were electrophoresed on 7.5–15% gradient SDS–polyacrylamide gels that were fixed in 50% methanol/10% acetic acid, dried at 70°C and exposed to x-ray film for detection of [^{32}P]-labeled myosin light chains. Labeled bands that corresponded to the HUVE regulatory myosin light chains were cut from the SDS–polyacrylamide gel and digested with TPCK-treated trypsin as outlined by Ludowyke et al. (48).

Tryptic peptides of HUVE myosin light chains were separated following the methods described by Daniel and Sellers (14). Standards for one-dimensional tryptic peptide maps were generated by in vitro phosphorylation of HUVE myosin. Protein A beads containing immune complexed HUVE myosin II were incubated with MLCK as outlined by Umemoto et al. (67) or with protein kinase C as described by Kawamoto et al. (40) for 15 min at 30°C. Phosphorylation was terminated by addition of 1 ml of PBS containing 25 mM EGTA (pH 7.4) followed by three 1-ml washes in PBS. Protein A–Sepharose beads were resuspended in 100 μl of SDS sample buffer (44) and phosphorylated myosin II electrophoresed on 7.5–15% gradient SDS–polyacrylamide gels.

Actin Quantitation

Monolayers were fixed in freshly prepared 3% formaldehyde in stabilization buffer (SB; 127 mM NaCl, 50 mM KCl, 1.1 mM NaH_2PO_4, 2 mM Mg_2SO_4, 1 mM EGTA, 20 mM Pipes, 5.5 mM glucose, pH 6.5) at 37°C for 10 min and for an additional 50 min at room temperature. The fixed cultures were washed twice with SB and then permeabilized in SB containing 0.1% NP-40, 0.05% DOC for 15 min. Permeabilized monolayers were stained in the dark with 0.175 μg rhodamine phalloidin in PBS for 60 min at room temperature and then gently washed three times with SB. Cultures were extracted with 1.5 ml of methanol for 2 h; cytoskeletons washed with an additional 0.5 ml methanol, samples combined, and rhodamine phalloidin content quantitated using a SLM 8100 fluorospectrophotometer (exitation 542 nm, emission 563 nm).

To quantitatively express the changes in F-actin, it was necessary to compensate for variability in cell number among cultures. Previous studies (5, 22) have used ethidium bromide to stain cells and reported the difference in fluorescent intensity per culture was a reflection of nuclear staining, hence, variations in cell number. Our initial studies following published protocols (22) found ethidium bromide staining to be nonspecific. For these studies we used a DNA fluorochrome that is highly DNA specific. The probe is prepared following the methods outlined by Lundell and Hirsh (49).

After methanol extraction of rhodamine phalloidin, monolayers were rehydrated in three washes of DPBS for a total of 15 min. Cultures were then flooded with 1.5 ml of working fluoroprobe and endothelial cytoskeletons removed from the dish with a rubber policeman. Dishes were washed with an additional 500 μl of the fluoroprobe, samples combined and sonicated in a bath sonicator for three 5-s bursts. Fluorescent intensity was measured with an SLM-Aminco 8100 fluorospectrophotometer (exitation 466 nm, emission 565 nm, bandpass of 4, 0.5 s integration, with a PMT setting of 600V). The fluorescence intensity (FI) was expressed as a ratio of extracted rhodamine phalloidin fluorescence to DNA fluorescence to correct for variation in cell number among cultures. Results are then expressed as relative F-actin content (RFC); i.e., the ratio of FI thrombin to FI control ($RFC = FI_{thrombin}/FI_{control}$).

HUVE Myosin II Distribution

Stimulation media was aspirated and cultures flooded with 1 ml of 37°C permeabilization buffer B (20 mM Pipes, 10 mM Imidizole, 50 mM KCl, 25 mM $Na_4P_2O_7$, 25 mM NaF, 0.1% Triton X-00, 0.05% NP-40, 0.2 mM PMSF, 100 μg/ml benzamidine, 100 μg/ml soybean trypsin inhibitor, 10 μg/ml of TPCK, TLCK, aprotinin, leupeptin, and pepstatin pH 6.5) for 30 s at room temperature. Buffer B (containing the soluble myosin II fraction) was then aspirated and spun at 12,000 *g*, 4°C for 2 min to ensure removal of any floating cells. The recovered volume from each culture dish was determined and the differences in recovery corrected for before gel analysis. A 200-μl aliquot was removed from the soluble myosin II fraction, added to 100 μl of boiling 3× SDS sample buffer and heated at 100°C for an additional 5 min. The samples were subjected to SDS–polyacrylamide gel electrophoresis in 7.5% vertical slab gels using the buffer system of Laemmli (44) and the proteins were transferred to 0.2-μm nitrocellulose membrane at 90 mAmp at 4°C for 20 h in 25 mM Tris, 192 mM glycine, 0.1% SDS, and 20% methanol, pH 8.3. Myosin II was detected by the ECL method (Amersham Corp., Arlington Heights, IL) using an affinity-purified rabbit antibody to human platelet myosin II heavy chain. X-ray films were developed at various time intervals to obtain an exposure within the linear range of the film. Films were scanned in a personal densitometer (Molecular Dynamics, Sunnyvale, CA) in two dimensions; the densitometry units (DU) for each sample were standardized based on DNA content (see below) and expressed as a ratio of densitometric units to DNA content. Results are then expressed as relative myosin II content (RMIIC); i.e., DU thrombin to DU control. ($RMIIC = DU_{thrombin}/DU_{control}$).

DNA content was determined following a modification of the procedure described by West et al. (69). Following aspiration of buffer B, cultures were immediately flooded with 1.0 ml of 10 mM EDTA, pH 12.3, containing 50 μg/ml RNase (DNase-free) and incubated at 37°C for 20 min. After incubation cultures were cooled to 4°C on ice, cytoskeletons scraped up with a rubber policeman, and transferred to 13 × 100-mm test tubes. Cultures were washed with an additional 400 μl 10 mM EDTA, pH 12.3, samples combined, sonicated in a bath sonicator and 100 μl of 1M KH_2PO_4 added to neutralize the pH. For fluorometric determination of DNA, 1.5 ml of Hoechst 33258 (200 ng/ml in 100 mM NaCl, 10 mM Tris, pH 7.0) was rapidly added to each tube and gently vortexed. Fluorescence was measured using a fluorescence spectrophotometer (slit width 5, sensitivity 0.3, excitation 350 nm, and emission 455 nm; 650-10s; Perkin-Elmer Cetus Instrs., Norwalk, CT). Standards of salmon testes DNA were added directly to 1.4 ml of 10 mM EDTA, pH 12.3, incubated at 37°C for 20 min and treated identically to experimental samples.

Immunofluorescence

For fluorescent staining, cells were grown in 35 × 10-mm fibronectin coated culture dishes. To visualize actin microfilaments, control and treated monolayers were fixed with freshly prepared 3% formaldehyde in SB, pH 7.0, stained with rhodamine phalloidin (Molecular Probes, Inc., Eugene, OR) by the method of Barak et al. (3), washed with PBS, and coverslipped in 90% glycerol/10% PBS containing 0.1M *n*-propyl gallate (20). For myosin II staining, cultures were fixed in 37°C 1% formaldehyde

in SB, pH 6.5, for 60 s followed by fixation and permeabilization in 2% formaldehyde/SB containing 0.2% Triton X-100, 0.5% DOC for an additional 60 min at room temperature. Cultures were gently washed in SB and further permeabilized by incubation in 0.4% Triton X-100, 0.6% DOC for 5 min. Monolayers were rinsed in SB and then incubated for 2 min in 10 mM sodium borohydrate to reduce free aldehyde groups. Nonspecific binding was minimized by incubation of cultures in blocking buffer (PBS containing 0.8% BSA, 0.1% gelatin, 10 μg/ml normal goat IgG, pH 7.3) for 1 h at room temperature. HUVE were stained with an affinity-purified rabbit anti-human platelet myosin II heavy chain antibody for 1 h and then with affinity-purified rhodamine conjugated goat anti-rabbit IgG antibody for an additional 60 min. Cultures were washed in PBS and coverslipped with 90% glycerol/10% PBS containing 0.1 M *n*-propyl gallate. Z-series were performed with a Bio-Rad MRC600 Confocal Microscope and composite micrographs constructed.

Affinity Antibody Purification

A rabbit polyclonal IgG fraction (15 mg/ml) that was reactive against HUVE myosin II heavy chains was purified against human platelet myosin II. Platelet myosin II (14) (1 mg/ml) was coupled to cyanogen-bromide-activated Sepharose 4B (Sigma Chem. Co., St. Louis, MO) for 6 h at room temperature. After extensive washing and equilibration in PBS, rabbit IgG diluted 1:1 with PBS, pH 7.5, was applied to the myosin II affinity column. The antibody was recycled twice through the column. Beads were washed with PBS containing 0.4 M NaCl, equilibrated in PBS and then eluted with 0.2 M glycine, pH 3.0; followed by 1 bed vol of distilled water. Eluted fractions were brought to pH 7.0 with 1 M Tris pH 9.0, concentrated and dialyzed against PBS, pH 7.3, containing 1 mM NaN_3. Affinity-purified antibodies were stored at −70°C.

Results

Isometric Tension

The present study uses a second generation isometric tension apparatus (Fig. 1 *A*) that permits simultaneous measurements on two monolayers as well as multiple measurements (8 per week) because of the ability to prepare and maintain monolayers separate from the ITMA. The removable specimen platform (Fig. 1 *B*) was constructed such that the porous polyethylene holders are immobilized by alligator clips so that HUVE cells seeded onto precast collagen gels can compress the collagen gel into a thin membrane over the period of days needed to establish a stable basal tension. Without immobilization of the polyethylene holders, cell-populated ridges form in the center of the collagen gel as the endothelial cells compress and thin the gel, and with time the holders are pulled together. With the new design, monolayers grown on the RSP develop the same basal tension as those grown attached to the ITMA and they can be transferred and attached to the x, y, z micromanipulators and force transducers without slacking or stretching of the monolayers, changes that have been found to alter the response of HUVE monolayers to vasoactive mediators (unpublished observations).

Precast collagen gels prepared on either the ITMA or the RSP were seeded with HUVE cells at densities that formed a confluent monolayer within 6 h and compressed the collagen gel into a thin membrane over the following 2–3 d. A stable isometric tension of 30–35 dynes (33 ± 3.5, $n = 9$) developed within 5–6 d of confluence and remained stable for up to 21 d. Monolayers were used within 24 h of reaching a steady basal tension (typically 8 d after seeding) however, no variation in response was detected in monolayers used up to 10–15 d after seeding. After stimulation, monolayers were washed with MCDB-107 containing 0.25% BSA and basal tension was allowed to restabilize for 60 min. Fig. 2 depicts a typical tracing of isometric tension produced by a HUVE monolayer exposed to 1 U/ml thrombin. Isometric tension developed rapidly within the first minute and reached a peak of 59 dynes by 5 min. Peak tension was maintained for 50 min before slowly declining over the following 60 min. Although the time course and magnitude of tension development was consistent among preparations, variations occurred in the duration of maximally sustained tension. Thrombin treated monolayers achieved a peak tension of 60.5 ± 4.5 ($n = 9$) dynes within 5 min while the duration of sustained tension varied from 50 to 80 min. Addition of 3 μM cytochalasin D at any time during the experiment rapidly abolished the isometric tension produced by the monolayers. No differences in tension development were evident when using monolayers grown external to the ITMA.

HUVE Myosin Light Chain Phosphorylation and Isometric Tension Development

For determination of the dose dependence of thrombin induced myosin light chain phosphorylation, cultures were labeled with [^{32}P]orthophosphoric acid, incubated with various concentrations of thrombin for 5 min and myosin II immunoprecipitated and the extent of myosin light chain phosphorylation assessed as described previously (73). Thrombin treatment results in a dose-dependent increase in myosin light chain phosphorylation (data not shown). A 1.7-fold increase in myosin light chain phosphorylation occurred with 0.1 U/ml thrombin and phosphorylation increased with each successive dose reaching maximal levels, over three times that of controls, at 0.75 U/ml thrombin. No significant increase in myosin heavy chain phosphorylation was detected over control cultures (data not

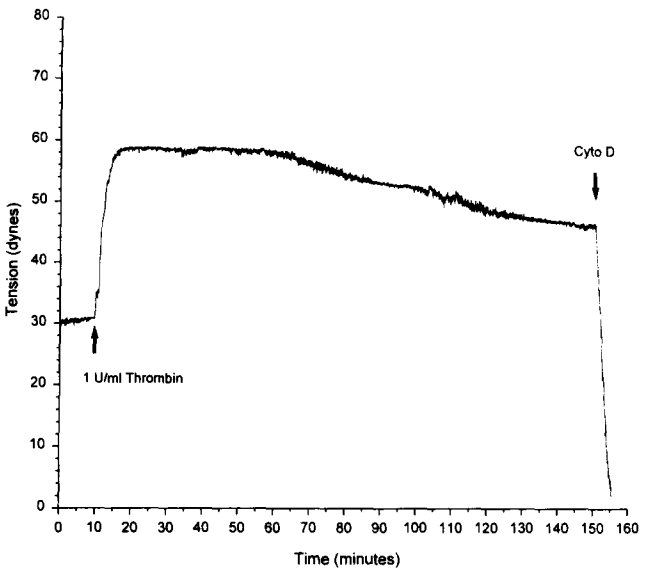

Figure 2. Representative tracing of isometric tension produced by HUVE exposed to 1 U/ml thrombin. Thrombin causes a rapid rise in tension reaching a peak of 59 dynes. Peak tension is maintained for 50 min before slowly declining over the ensuing 60 min. Treatment with 3 μM cytochalasin D abolished tension within 5 min.

shown). Based upon these results, a dose of 1 U/ml thrombin was chosen for all experiments. The doses of thrombin found to elicit an increase in light chain phosphorylation are within the range observed during blood clotting (61) implicating thrombin as a potential physiological mediator of endothelial cell contraction.

To characterize myosin light chain phosphorylation induced by thrombin in HUVE cells, two-dimensional electrophoretic studies were performed. In the first set of experiments, monolayers were labeled with either [^{35}S]methionine or double labeled with [^{35}S]methionine and [^{32}P]-orthophosphoric acid as outlined under Materials and Methods. Cultures were stimulated for the desired time intervals, myosin II immunoprecipitated and then separated by two-dimensional gel electrophoresis with IEF (pH 4–6) in the first dimension and SDS-PAGE in the second dimension. SDS-PAGE gels were dried and exposed to phosphor screens. Fig. 3, *A* and *B* show images of immunoprecipitated myosin II from a double labeled culture illustrating the separation of unphosphorylated and phosphorylated forms of HUVE myosin light chains. To distinguish between the [^{32}P]- and [^{35}S]-labeled light chains, SDS PAGE gels were exposed to the phosphor screen as follows: (*a*) a copper foil (0.0014 in thick; All-Foils, Brooklyn Heights, Ohio) was placed between the dried gel and the phosphor screen effectively blocking the beta emissions and allowing detection of only the [^{32}P]-labeled light chains (Fig. 3 *A*) and (*b*) gels were reexposed directly to phosphor plates to detect both [^{32}P]- and [^{35}S]-labeled light chains (Fig. 3 *B*). By double labeling myosin II and differentially exposing the same gel, we were able to identify without ambiguity the unphosphorylated and phosphorylated myosin light chains. Fig. 3 *A* shows the presence of two [^{32}P]-labeled myosin light chain isoforms (M_1, M_2; D_1, D_2) that correspond to the 18- (M_2, D_2) and 19-kD (M_1, D_1) light chains each of which exists in two phosphorylation states, i.e., monophosphorylated and diphosphorylated. The monophosphorylated light chains focus closer to the cathode (M_1, M_2) and the diphosphorylated to the anode (D_1, D_2). Fig. 3 *B* is a direct exposure of the same gel that detects both [^{32}P]- and [^{35}S]-labeled light chains. In addition to the phosphorylated light chains, this image shows the unphosphorylated forms of each myosin light chain isoform (U_1,U_2) that separate as the most basic proteins. The nonphosphorylatable light chains (NP) were also detected; these also exist as isoforms and have molecular masses of 16 (NP_1) and 15.5 kD (NP_2). The apparent isoelectric points of the phosphorylatable and nonphosphorylatable myosin II light chain isoforms are listed in Table I.

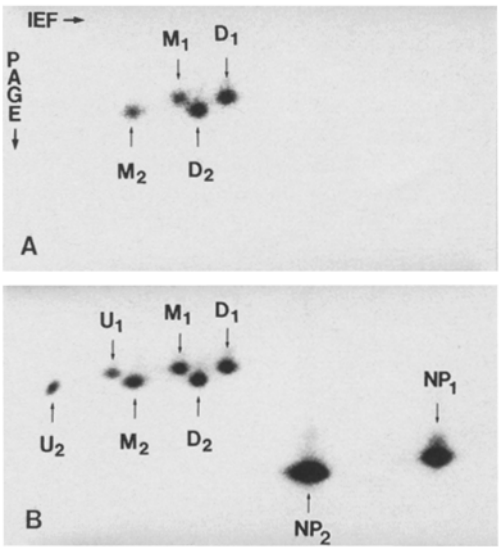

Figure 3. Phosphor images demonstrating two-dimensional gel electrophoretic separation of unphosphorylated and phosphorylated isoforms of HUVE myosin light chains. Cells were labeled with both [^{35}S]methionine and [^{32}P]orthophosphoric acid, stimulated with 1 U/ml thrombin for 2.5 min at 37°C and myosin II immunoprecipitated as described in Materials and Methods. Myosin II was then subjected to IEF (pH 6–4) in the first dimension and 15% SDS PAGE in the second dimension. (*A*) SDS PAGE gel exposed to a phosphor screen through a copper foil to block beta emissions allowing discrimination between [^{32}P]- and [^{35}S]-labeled light chains. Two [^{32}P]-labeled myosin light chain isoforms are detectable and exist in two phosphorylation states: monophosphorylated (M_1, M_2) and diphosphorylated (D_1, D_2). (*B*) Direct exposure of the SDS PAGE gel to the phosphor screen detects both [^{32}P]- and [^{35}S]-labeled myosin light chains. Two isoforms exist in unphosphorylated (U_1, U_2), monophosphorylated (M_1, M_2) and diphosphorylated (D_1, D_2) states with distinct isoeletric points. In addition, the two [^{35}S]-labeled nonphosphorylatable (NP_1, NP_2) myosin light chains were detected. Double labeling of cells and differential detection of radiolabeled proteins allows for direct identification of the relative mobility of the three myosin light chain phosphorylation states.

After establishing the relative positions and apparent isoelectric points of unphosphorylated and phosphorylated myosin light chains, changes in phosphorylation of [^{35}S]methionine-labeled myosin light chains were calculated to determine the stoichiometry of thrombin induced phosphorylation. Fig. 4 illustrates representative autoradiograms from selected time intervals after stimulation with 1 U/ml thrombin. Autoradiograms (Fig. 4) or phosphor images were analyzed by two-dimensional laser densitometry and the relative proportions of unphosphorylated, monophosphorylated, and diphosphorylated light chains determined as a percent of the total. The extent of myosin light chain phosphorylation was also calculated as moles of phosphate incorporated per mole of light chain. Quantitative data from six time course experiments is presented in Table II. In unstimulated cultures (Fig. 4 *A*, Table II), 57% of myosin light chains are unphosphorylated, 32% are monophosphorylated, and 11% are diphosphory-

Table I. Apparent Isoelectric Points of HUVE Myosin Light Chain Isoforms

Unphosphorylated	
U_2	5.11
U_1	5.07
Monophosphorylated	
M_2	5.04
M_1	5.01
Diphosphorylated	
D_2	4.99
D_1	4.95
Nonphosphorylatable	
NP_2	4.86
NP_1	4.77

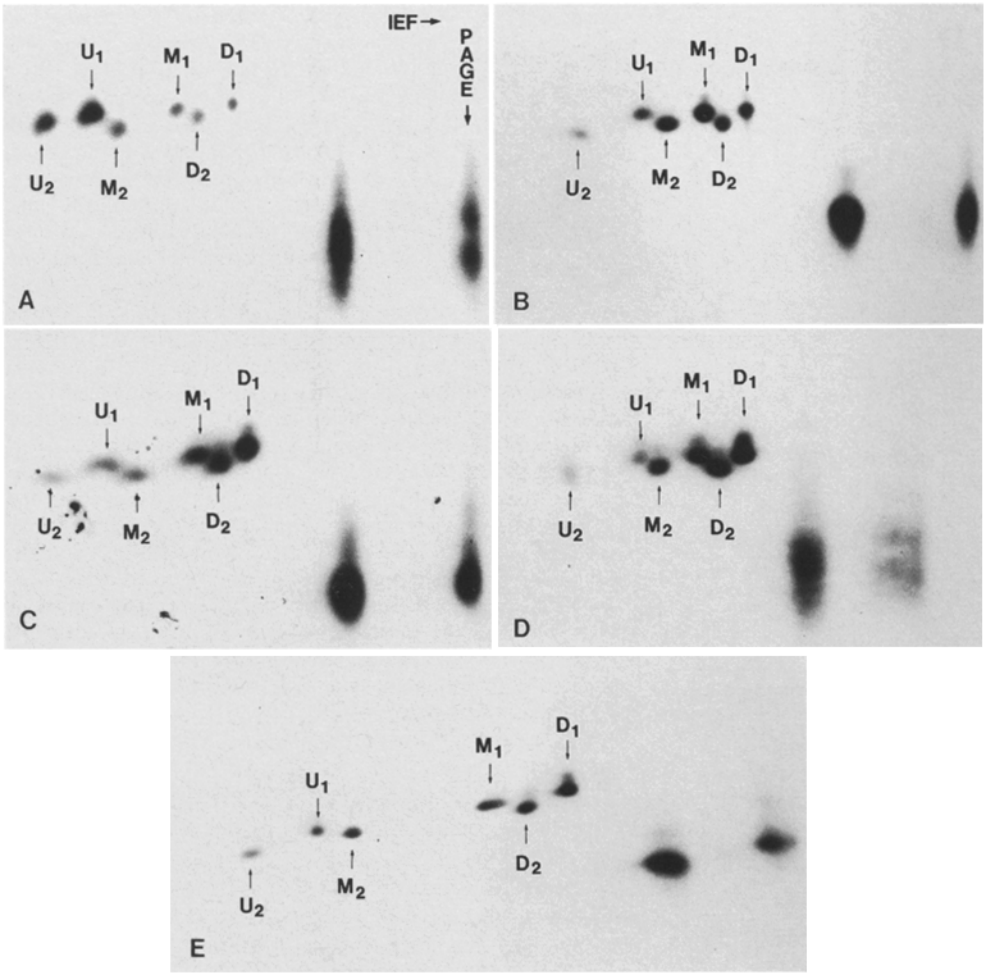

Figure 4. Two-dimensional analysis of myosin light chain phosphorylation from control (*A*) and thrombin stimulated (*B–E*) cultures. HUVE cells were labeled with [^{35}S]methionine as described in Materials and Methods and incubated with 1 U/ml thrombin for 30 s (*B*), 2.5 min (*C*), 30 min (*D*), and 60 min (*E*). Myosin II was immunoprecipitated and analyzed by two-dimensional electrophoresis to determine the change in unphosphorylated and phosphorylated forms of HUVE myosin light chain isoforms. Representative time points illustrating major shifts in phosphorylation states are presented. Quantitative data from the entire time course of myosin light chain phosphorylation is presented in Table II. Only those portions of the gels that include the regulatory and essential light chains are shown.

lated. After 30 s (Fig. 4 *B*, Table II) of thrombin stimulation, the amount of unphosphorylated light chains decreased to 16% while the monophosphorylated and diphosphorylated increased to 45 and 39%, respectively. By 60 s (Fig. 4 *C*, Table II) maximal levels of phosphorylation were achieved with 66% of the myosin light chains diphosphorylated, 29% monophosphorylated, and only 5% remaining unphosphorylated. This level of phosphorylation was maintained up to 30 min (Fig. 4 *D*, Table II) after the addition of thrombin. After 60 min (Fig. 4 *E*, Table II) in the continued presence of thrombin, diphosphorylated myosin light chains fell to 48% with concomitant increases occurring in both the mono- and unphosphorylated states; this represents a 12.5% reduction in light chain phosphorylation. Analysis of the 18- and 19-kD light chain isoforms revealed no significant difference between their time course and extent of phosphorylation.

Fig. 5 compares the stoichiometry of myosin light chain phosphorylation with tension development. The mean results of six different experiments are presented. Basal tension is associated with 0.54 ± 0.06 mol PO_4/mol of MLC. Maximal phosphorylation of 1.61 ± 0.12 mol PO_4/mol of MLC occurs within 60 s while tension develops more gradually reaching maximal levels by 5 min. The rise in tension parallels the rise in phosphorylation although maximal phosphorylation precedes maximal tension development

Table II. Distribution and Stoichiometry of Myosin Light Chain Phosphorylation in Control and Thrombin Stimulated HUVE Monolayers

	Cont	30 s	60 s	2.5 min	15 min	30 min	60 min
Unphosphorylated ($U_1 + U_2$)	57 ± 5	16 ± 6	5 ± 2	8 ± 5	12 ± 5	12 ± 7	23 ± 8
Monophosphorylated ($M_1 + M_2$)	32 ± 5	45 ± 5	29 ± 7	24 ± 11	24 ± 8	21 ± 6	29 ± 2
Diphosphorylated ($D_1 + D_2$)	11 ± 2	39 ± 2	66 ± 10	68 ± 13	64 ± 13	67 ± 9	48 ± 9
mol PO_4/mol MLC	0.54 ± 0.06	1.23 ± 0.07	1.61 ± 0.12	1.59 ± 0.17	1.53 ± 0.18	1.56 ± 0.15	1.25 ± 0.17

Cultures were labeled with [^{35}S]methionine, stimulated with thrombin, and myosin II immunoprecipitated. The light chain isoforms/phosphorylation states were separated by two-dimensional electrophoresis and the percentage of unphosphorylated ($U_1 + U_2$), monophosphorylated ($M_1 + M_2$), and diphosphorylated ($D_1 + D_2$) myosin light chains determined by laser densitometric scans of autoradiograms (Fig. 4) or phosphor image analysis. The stoichiometry of myosin light chain phosphorylation (mol phosphate/mol MLC) was calculated from the percentage of monophosphorylated and diphosphorylated myosin light chains as described in Materials and Methods. Each point is the mean ± SE of six separate experiments.

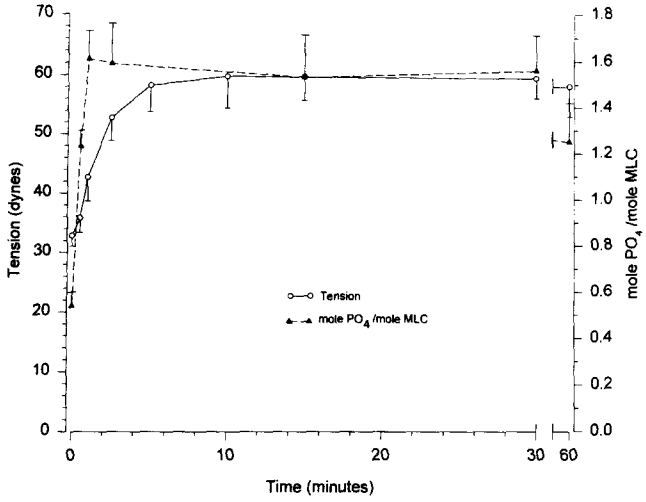

Figure 5. Time course of isometric tension and stoichiometry of myosin light chain phosphorylation upon exposure to 1 U/ml thrombin. The extent of tension (Fig. 2) and phosphorylation (Fig. 4, Table II) were determined at 30 and 60 s, 2.5, 15, 30, and 60 min. The increase in phosphorylation (mol PO_4/mol MLC) precedes the development of isometric tension, but by 60 s phosphorylation parallels tension development. Myosin light chain phosphorylation peaks at 60 s and remains elevated during the sustained phase of isometric tension. By 60 min, both tension and myosin light chain phosphorylation begin to decline with phosphorylation declining more rapidly than tension. Each point is the mean ± SE of six separate experiments.

(Fig. 5). Maximal phosphorylation and tension were achieved within 5 min and remain at peaked levels for 30 min. By 60 min, both tension and phosphorylation begin to decline with phosphorylation decreasing more rapidly than tension.

Identification of Phosphorylation Sites in HUVE Myosin Light Chains

To determine if MLCK or PKC was responsible for the thrombin induced increase in myosin light chain phosphorylation, the sites of in vivo phosphorylation were analyzed by one-dimensional tryptic phosphopeptide mapping. For a direct comparison, HUVE light chains were phosphorylated in vitro by either MLCK (Fig. 6, lane *1*) or by PKC (Fig. 6, lane *5*). The in vitro phosphorylated HUVE light chains were then subjected to the same tryptic digestion as thrombin stimulated samples. Fig. 6 illustrates the phosphopeptide map of thrombin induced phosphorylated myosin light chains (lanes *2–4*) and the in vitro phosphorylated standards (lanes *1* and *5*). The tryptic map of the MLCK phosphorylated standard (lane *1*) consisted of two phosphopeptides. MLCK phosphorylated Ser-19 that corresponds to the lower more basic phosphopeptide present in lane *1*. In addition, MLCK phosphorylated Thr-18 resulting in a diphosphorylated peptide (Ser-19/Thr-18) that migrates to a more acidic position on the one-dimensional IEF gel. The tryptic map of the PKC phosphorylated HUVE myosin light chain standards (Fig. 6, lane *5*) revealed three phosphopeptides. The two acidic peptides designed as Ser-1′ and Ser-1 have been shown to consist of the following sequences; Ser-1′ = *N*-acetyl-Ser-Ser-Lys and Ser-1 =

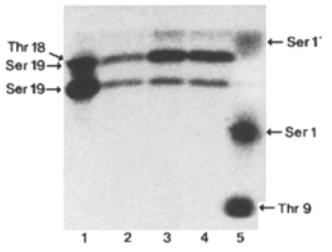

Figure 6. One-dimensional tryptic peptide map of HUVE myosin light chain phosphorylation sites. Monolayers were labeled with [^{32}P]orthophosphoric acid; myosin II was immunoprecipitated from control (lane *2*) and stimulated cultures (lanes *3* and *4*), digested with trypsin, and labeled phosphopeptides separated by one-dimensional isoelectric focusing gel electrophoresis. HUVE myosin light chains were phosphorylated in vitro by MLCK (lane *1*) or by PKC (lane *5*) and used as standards. Ser-19 and Thr-18, (lane *1*) are sites for MLCK phosphorylation, while Ser-1, Ser-1′ and Thr-9 (lane *5*) are sites phosphorylated by PKC. Myosin light chains from control cultures exhibit constitutive phosphorylation at Ser-19 and Ser-19/Thr-18 sites that correspond to MLCK phosphorylation. Furthermore, myosin light chains from cultures incubated with thrombin for 2.5 min (lane *3*) and 60 min (lane *4*) are phosphorylated at Ser-19 and Ser-19/Thr-18. No PKC (lane *5*) phosphorylation was detected in control or stimulated cultures. Lane *1*: in vitro phosphorylation of HUVE myosin light chains by MLCK; lane *2*: in vivo phosphorylation from control monolayers; lanes *3* and *4*: in vivo phosphorylation from HUVE monolayers stimulated with thrombin; lane *5*: in vitro phosphorylation of HUVE myosin light chains by PKC.

N-acetyl-Ser-Ser-Lys-Arg (14, 54). PKC phosphorylation of the Thr-9 corresponds to the most basic phosphopeptide in lane *5*.

Tryptic phosphopeptides obtained from control (lane *2*) and stimulated monolayers (lanes *3* and *4*) comigrated with the bands produced by phosphorylation of HUVE myosin light chain standards by MLCK (lane *1*). Unstimulated cultures exhibited basal phosphorylation that corresponds to both monophosphorylated (Ser-19) and diphosphorylated (Ser-19/Thr-18) phosphopeptides. Stimulation with 1 U/ml thrombin for 2.5 min (lane *3*) or 60 min (lane *4*) produced increases in [^{32}P] incorporation into both phosphopeptides although the largest increase occurs in the diphosphorylated peptide (Ser-19/Thr-18). Phosphopeptides corresponding to the residues phosphorylated by PKC were not detected in either control or stimulated monolayers. Qualitatively the data obtained by one-dimensional tryptic peptide mapping is in agreement with the analysis of myosin light chain phosphorylation states obtained by two-dimensional analysis of [^{35}S]methionine-labeled monolayers (Table II).

Thrombin Stimulated Reorganization of Actin and Myosin II

After demonstrating that the increase in isometric tension in thrombin stimulated HUVE monolayers parallels myosin light chain phosphorylation, confocal microscopy was used to examine the morphological changes in F-actin and myosin II. Monolayers were treated with 1 U/ml thrombin for various times, were fixed and stained for F-actin with rhodamine phalloidin or for myosin II with affinity-purified rabbit anti–human platelet myosin II heavy chain antibody as outlined under Materials and Methods. Fig. 7 shows Z-series composite micrographs of control and thrombin stimulated HUVE monolayers. Fig. 7 *A* illus-

trates the F-actin distribution and Fig. 7 *G* the myosin II distribution from control monolayers grown on fibronectin-coated culture dishes. Monolayers consist of a cohesive sheet of polygonal cells exhibiting a thin rim of F-actin staining at their margins. HUVE are devoid of prominent stress fibers. However, most cells contain a few randomly dispersed fibers, while myosin II (Fig. 7 *G*) is diffusely localized throughout the cytoplasm with no obvious organization. With thrombin stimulation, both F-actin and myosin II undergo rapid and striking redistribution. Fig. 7 shows the F-actin (*B–F*) and myosin II (*H–L*) distributions in HUVE monolayers treated with 1 U/ml thrombin for 30 and 60 s, 2.5, 30, and 60 min, respectively. By 30 s (Fig. 7 *B*), a fine latticework of F-actin is evident throughout the cell cytoplasm. Distinct margins that delineate cells are no longer evident as the monolayer assumes the appearance of a contiguous meshwork of filaments. Myosin II (Fig. 7 *H*) changes from the diffuse amorphous distribution present in control cells and organizes into discrete aggregates dispersed randomly throughout the cytoplasm. By 60 s (Fig. 7 *C*), the underlying latticework of F-actin is still present but organizing stress fibers begin to predominate. Myosin II (Fig. 7 *I*) still localizes as discrete aggregates although there appears to be a more intense generalized staining than is seen at 30 s.

By 2.5 min (Fig. 7 *D*) the actin filaments form an interconnecting cross-linked network of stress fibers that fills the cytoplasm. The filaments appear to radiate from discrete foci (*arrows*) of condensed F-actin localized at cell margins. Myosin II (Fig. 7 *J*) colocalizes to actin filaments and exhibits a periodic distribution. Concentrations of myosin II are evident at the cell margins (*arrows*) and coincide with foci of condensed F-actin filaments. After 30 min (Fig. 7 *E*), the actin has reorganized into prominent stress fibers aligned parallel to each other and to the long axis of the cell. Cells have retracted from one another, exhibiting small gaps between adjacent cells while retaining their polygonal morphology. Contracted HUVE cells remain attached to one another by slender cell processes containing F-actin filaments. In many areas, the stress fibers appear to be contiguous between adjacent cells. This same reorganized actin configuration is detected after 60 min of stimulation (Fig. 7 *F*). HUVE myosin II associates in a periodic band-like pattern with the underlying actin stress fibers at both 30 (Fig. 7 *K*) and 60 min (Fig. 7 *L*). The inset in Fig. 7 *L* clearly illustrates the sarcomeric-like myosin II distribution in stimulated cells. In most cells, myosin II is excluded from the peripheral cytoplasm and the majority of slender actin containing cell processes that connect adjacent cells.

HUVE F-actin content was then quantitated by methanol extraction of rhodamine phalloidin stained cultures. Actin was standardized to DNA content to correct for variations in cell number among dishes and experiments. Fig. 8 illustrates the time course of thrombin induced increases in F-actin content. Thrombin stimulated actin polymerization rapidly increased by 20% within 30 s and achieved maximal levels 58% above unstimulated controls within 90 s. A slight drop in total F-actin content was detected at 5 min, however these levels were maintained at 30 min. By 60 min a 12% reduction in total F-actin content was seen.

Redistribution of HUVE myosin II to the detergent insoluble cytoskeleton paralleled changes that occurred in total F-actin. Thrombin stimulated cells were extracted with buffer B and the myosin II in the detergent soluble fraction (cytoplasmic) was quantitated by Western blotting. Detergent insoluble fractions (cytoskeleton) were extracted with 10 mM EDTA, pH 12.3, and DNA content measured as described under Materials and Methods. In unstimulated HUVE cultures, 88 ± 2.8% ($n = 7$) of the total cellular myosin was present in the detergent soluble or cytoplasmic fraction. In all experiments, the cytoplasmic myosin II value in unstimulated cultures was designated as 1.0 and the loss of myosin II from this fraction was used as a measure of myosin II association with the detergent insoluble fraction. This was confirmed in several experiments by either quantitating both cytoplasmic myosin II as well as cytoskeletal associated myosin II or by immunofluorescent staining of myosin II. All data was normalized to total DNA content. Fig. 9 shows the time course of the change in cytoplasmic myosin II following stimulation with 1 U/ml thrombin. Within 30 s, 73% of myosin II was no longer present in the detergent soluble fraction. Maximal redistribution (95%) of myosin II occurred by 5 min. The myosin II in the detergent soluble fraction subsequently increased 22% over the ensuing 55 min.

Discussion

Active contraction of endothelial cells was first suggested by Majno et al. (51) in 1969 as the mechanism responsible for the permeability edema induced by histamine. Our previous studies provided evidence for Majno's hypothesis by demonstrating that endothelial cell retraction required permissive levels of ATP (72) and was associated with myosin light chain phosphorylation (73, 74). These studies also showed that removal or inhibition of MLCK in permeabilized preparations prevented retraction that could then be rescued by the addition of exogenous MLCK, Ca^{2+} and calmodulin (73). More recently in intact monolayers, we have shown that HUVE exposed to thrombin produce isometric tension (41). In this study, we demonstrate that isometric tension development correlates with myosin II light chain phosphorylation and is accompanied by polymerization and extensive reorganization of actin as well as association of myosin II with the detergent insoluble cytoskeleton. Furthermore, thrombin-induced myosin light chain phosphorylation is catalyzed by MLCK.

Experiments documenting tension development were performed on a second generation isometric monitoring apparatus. The design of the external specimen platform had to permit immobilization of the porous polyethylene holders to (*a*) prevent movement during basal tension development and (*b*) allow transfer to the ITMA without releasing developed tension or stretching the monolayer. Recent studies have documented the effects of stretch or stress relaxation on activation of Ca^{2+} channels (46, 70), actin polymerization (56, 63) and cAMP/PKA (26) signaling pathways. Consistent with these studies, we found that a moderate 5-dyne stretch induced actin polymerization in HUVE monolayers that takes 4–6 h to return to baseline and that movement of the collagen gel during basal tension development caused inconsistent results with agonist

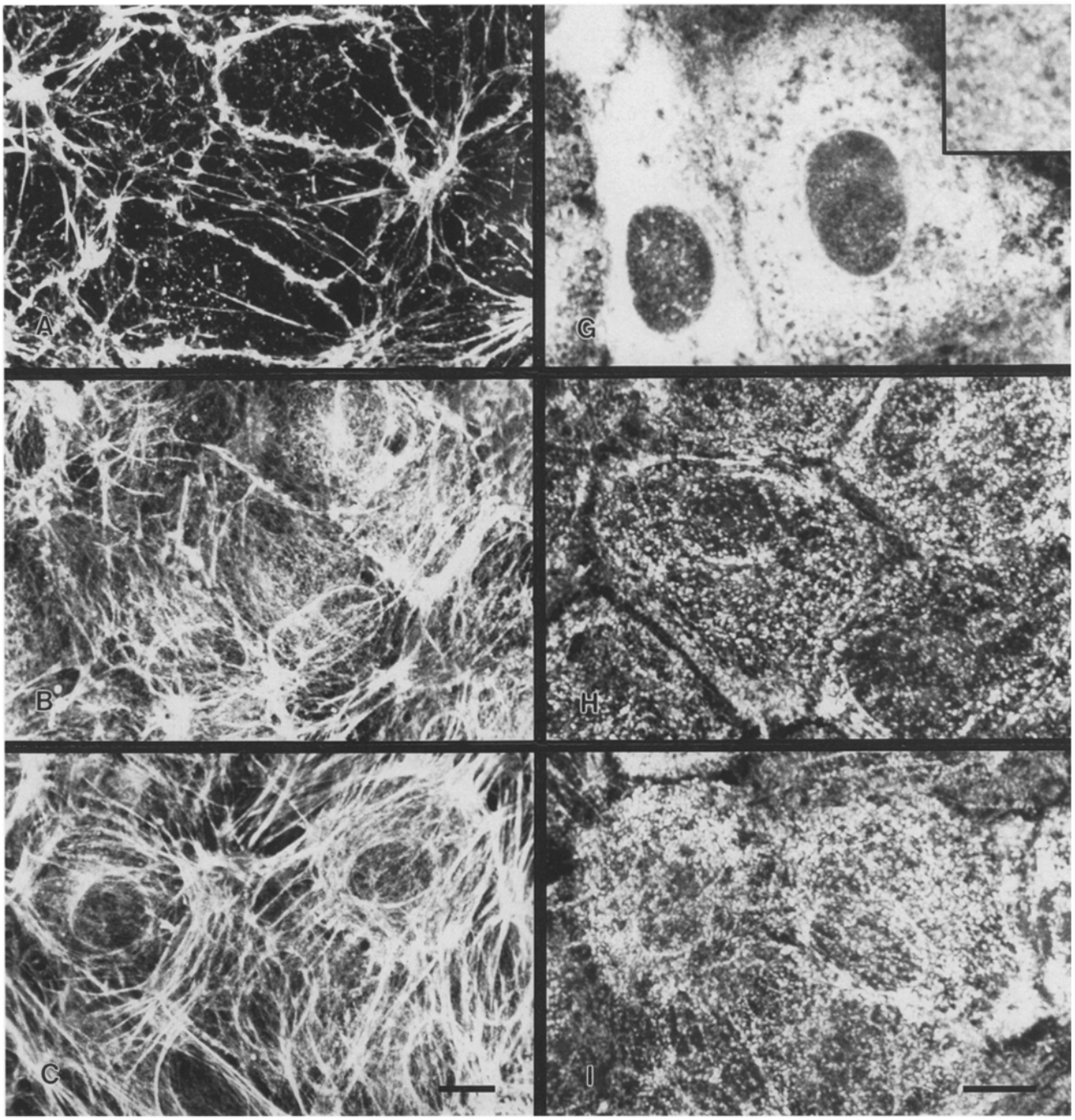

Figure 7. Immunofluorescent labeling in control and thrombin stimulated HUVE monolayers. Time course of redistribution of F-actin (*A–F*) and myosin II (*G–L*) upon exposure to 1 U/ml thrombin for 30 s (*B* and *H*), 60 s (*C* and *I*), 2.5 min (*D* and *J*), 30 min (*E* and *K*), and 60 min (*F* and *L*). F-actin was visualized by rhodamine phalloidin binding and myosin II was localized with affinity-purified anti-platelet myosin II antibodies as outlined in Materials and Methods. F-actin (*A*) and myosin II (*G*) distribution in unstimulated monolayers. A rim of F-actin staining is present at the cell margins with few randomly disoriented stress fibers within the cytoplasm. Myosin II is diffusely localized within the cytoplasm exhibiting no organized pattern. Upon thrombin stimulation, both F-actin (*B–F*) and myosin II (*H–L*) undergo progressive redistribution forming highly organized filamentous networks. Bar, 10 μm.

stimulation (unpublished observations). Cells seeded onto precast collagen gels develop a stable basal isometric tension within 5–6 d that is associated with constitutive light chain phosphorylation of 0.54 ± 0.06 mol PO_4/mol MLC. An increase in tension is detected within the first 30 s after thrombin stimulation reaching maximal levels within 5 min and maximal myosin II light chain phosphorylation (1.61 ± 0.12 mol PO_4/mol MLC) occurs at 60 s, preceding maximal tension development. Maximal phosphorylation is maintained throughout the sustained phase of isometric tension, and a decline in phosphorylation parallels the decrease in isometric tension. These data suggest that increases

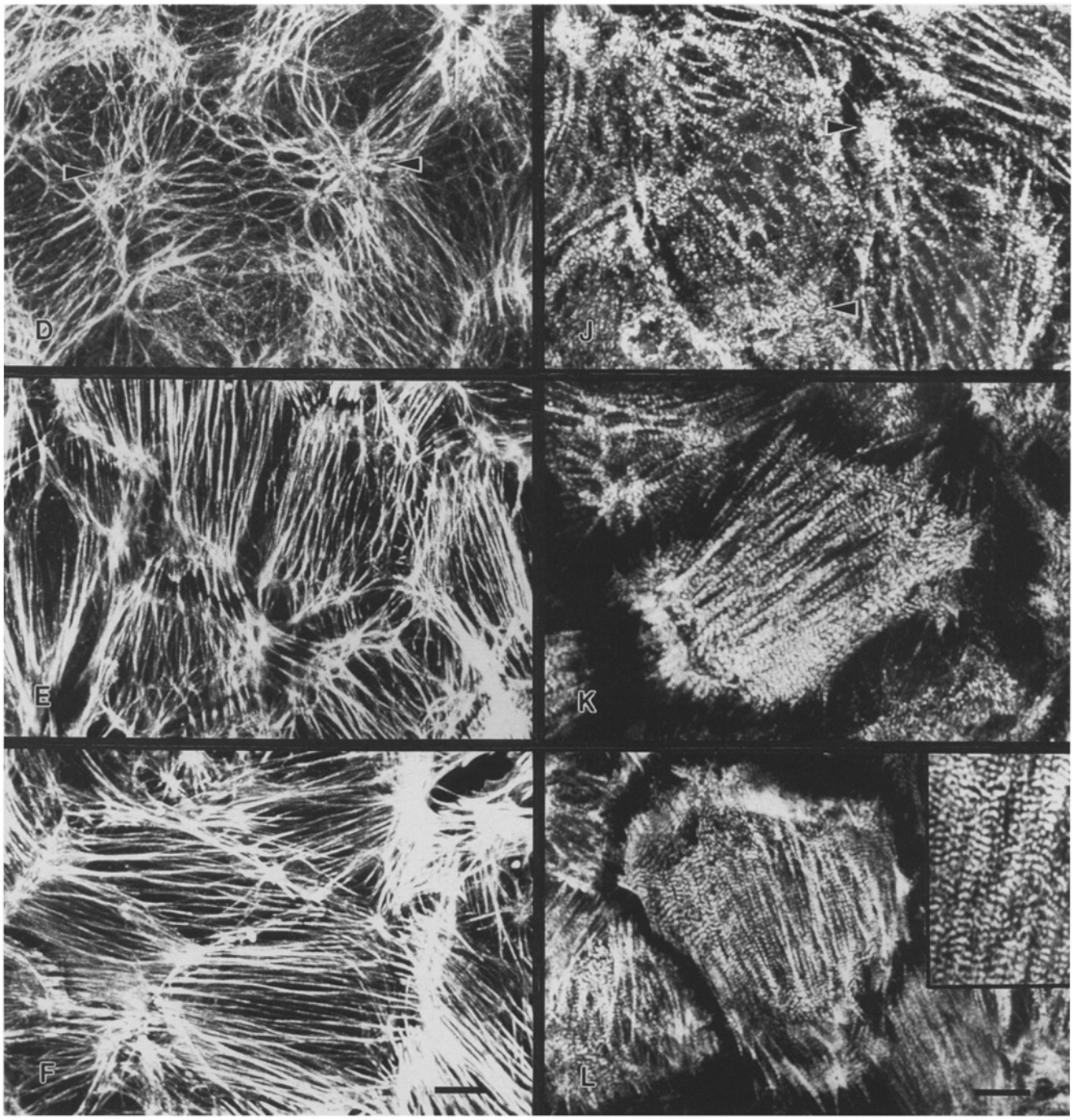

Figure 7.

in myosin II light chain phosphorylation initiate and sustain HUVE isometric tension.

Quantitation of the phosphorylation states of myosin II light chains was performed by two-dimensional (IEF/PAGE) gel electrophoresis. We found that HUVE phosphorylatable and nonphosphorylatable myosin light chains both consist of two isoforms with distinct molecular masses and isoelectric points (Table I). Isoforms of the phosphorylatable light chains have been identified in both smooth muscle (16, 39) and nonmuscle myosin (17, 40, 65). More recently, the cloning of cDNAs has been reported for smooth muscle and nonmuscle myosin (21, 43, 64). Both isoforms contain phosphorylation sites for both MLCK (Ser-19, Thr-18) and PKC (Ser-1, Ser-2, Thr-9) and since a high degree of homology exists between these isoforms, they are likely to be regulated in a similar fashion. In the present study, there was no significant difference in the degree of phosphorylation between the HUVE light chain isoforms. Although the functional significance of these light chain isoforms is not known, they may be associated with specific heavy chain isoforms (4) that constitute distinct myosin II pools within HUVE cells.

During the course of these studies, it became apparent that several factors significantly affected analysis of light

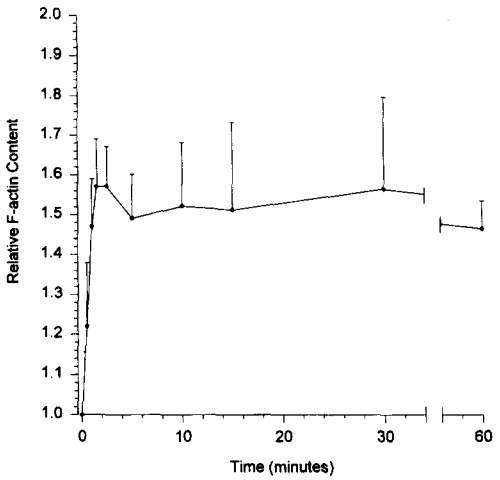

Figure 8. Time course of change in HUVE F-actin content after exposure to 1 U/ml thrombin. Monolayers were stimulated for 30, 60, 90 s, 2.5, 5, 10, 15, 30, and 60 min, fixed, permeabilized, and stained with rhodamine phalloidin. F-actin content was normalized to total cellular DNA as outlined in Materials and Methods. Results are expressed as relative F-actin content (RFC); the ratio of fluorescent intensity (FI) of stimulated cultures to fluorescent intensity of control cultures (RFC = $FI_{thrombin}/FI_{control}$). Each point is the mean ± SE of six separate experiments.

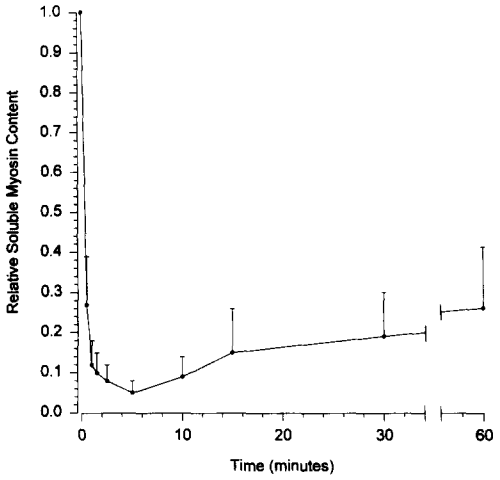

Figure 9. Time course of cytoplasmic myosin II association with the detergent insoluble cytoskeleton. HUVE monolayers were exposed to thrombin for the indicated time periods, permeabilized in buffer B, and processed as outlined in Materials and Methods. Cytoplasmic myosin II content was assessed by Western blotting using affinity-purified rabbit anti human platelet myosin II heavy chain antibodies. Detergent insoluble cytoskeletons were flooded with 10 mM EDTA, pH 12.3, for determination of DNA content. Cytoplasmic myosin II content in unstimulated cultures was designated as 1.0 and loss of myosin II from the soluble fraction used as a measure of myosin II association with the cytoskeleton. All data was normalized to DNA content and expressed as relative soluble myosin content as described in text. Each point is the mean ± SE of seven separate experiments.

chain phosphorylation in HUVE monolayers. To obtain reliable analysis of light chain phosphorylation, the following conditions had to be rigorously controlled: (*a*) post confluence of HUVE monolayers for at least 5 d; (*b*) maintenance of monolayers at 37°C before and during experiments; and (*c*) reextraction of the 132,000-*g* pellet to remove all phosphorylated myosin II.

Investigations of the mechanism of smooth muscle contraction have shown that agonist stimulation elicits increases in intracellular Ca^{2+}, myosin light chain phosphorylation, and force and that the former subsequently decline to low levels while developed force is maintained. In smooth muscle, force maintenance with reduced light chain phosphorylation and maximal shortening velocity has been referred to as the "latch state" and several studies (15, 24, 57) suggest that it results from attached dephosphorylated myosin crossbridges, i.e., latch bridges. It is hypothesized that latch bridges detach more slowly than phosphorylated crossbridges and thus may account for maintenance of force at low levels of myosin light chain phosphorylation (21, 24, 57).

In this study, the results of a comparison of the stoichiometry of myosin light chain phosphorylation and isometric tension is inconsistent with a latch state as the basis for isometric tension maintenance in thrombin stimulated HUVE monolayers. Our data is more consistent with maintenance of maximally phosphorylated crossbridges in the presence of a persistent signal. Reduction in tension is associated with a reduction of phosphorylated crossbridges. Though speculative, this explanation could account for the sustained tension induced by thrombin.

Initial experiments used [^{32}P]orthophosphoric acid-labeled monolayers to analyze light chain phosphorylation. An unexpected finding was the difference in quantitative phosphorylation data obtained with [^{32}P]orthophosphoric acid and [^{35}S]methionine in vivo labeling protocols. Time course experiments using [^{32}P]orthophosphoric acid-labeled cultures showed peak phosphorylation at 2.5 min with a 50% decline by 30 min (data not shown). In contrast, peak phosphorylation in [^{35}S]methionine-labeled cultures occurred at 60 s and was sustained for at least 30 min (Table II). Although there is no clear-cut explanation, the experimental conditions may account for these discrepancies. Since HUVE cells are extremely sensitive to prolonged exposure to phosphate-free media as well as high concentrations of [^{32}P]orthophosphoric acid, radiolabeling was performed in low phosphate media. This may interfere with either or both radiolabeling of ATP pools or maintenance of cellular ATP at a high specific activity for prolonged periods. To provide a reliable measure of the phosphorylation status of myosin II over time, the specific activity of the ATP pool used for phosphorylation must be constant. Changes in the specific activity or in the absolute ATP levels under the conditions used for these experiments could result in artifactual reduction in apparent phosphorylation. The physical separation of the [^{35}S]-labeled phosphorylated forms is expected to be far more reliable because of the stability of the label.

Unstimulated monolayers exhibit constitutively phosphorylated light chains with 57% un-, 32% mono-, and 11% diphosphorylated. Upon treatment with thrombin, a shift to the mono- and diphosphorylated light chains results and by 60 s the diphosphorylated (66%) light chains of both isoforms predominate. If HUVE tension develop-

ment is similar to that observed in smooth muscle, one would predict a close relationship between light chain phosphorylation and isometric tension, and indeed our data show that the presence of mono- and diphosphorylated light chains correlates with the time course of isometric tension development. Of interest is the fact that the persistence of diphosphorylated myosin II light chains parallels the time course of sustained isometric tension, and light chain dephosphorylation is accompanied by a decrease in isometric tension. Thus it appears that the diphosphorylated state of myosin light chains may be necessary for the maintenance of sustained HUVE isometric tension in contrast to smooth muscle.

Studies in vivo (8, 9, 11, 23) and in vitro (12, 31–33) have characterized site specific phosphorylation of myosin light chains, however, the functional significance of differential phosphorylation in vivo is unclear. Both smooth muscle and nonmuscle myosin II have multiple phosphorylation sites in their regulatory light chains. Two sites, the Ser-19 and Thr-18 residues, are phosphorylated by MLCK. The preferred site for MLCK phosphorylation is Ser-19, however, with high concentrations of MLCK, Thr-18 is also phosphorylated. The kinetics of site phosphorylation for both isolated light chains and intact myosin II are considerably different with Ser-19 500-fold more readily phosphorylated than Thr-18 (31, 33). Monophosphorylation by MLCK at Ser-19 in vitro has been shown to increase the actin-activated ATPase activity (1, 31–33), regulate myosin II filament assembly (12, 27, 32) and initiate motor activity of purified myosin in an in vitro motility assay (67). Diphosphorylation at Ser-19/Thr-18 increases myosin II filament stability and further increases actin-activated ATPase activity above that attributed to monophosphorylation at Ser-19, although there is no greater movement of diphosphorylated myosin in an in vitro motility assay (67). It is generally accepted that phosphorylation of myosin II light chains at Ser-19 by MLCK is responsible for the initiation of smooth muscle contraction. In smooth muscle tissue treated with high concentrations of carbachol (9) or by neuronal stimulation (52), low levels of diphosphorylated myosin light chains are found transiently (11 and 5%, respectively) and are considered physiologically insignificant in terms of smooth muscle contraction. Furthermore, studies in permeabilized smooth muscle preparations have shown that monophosphorylation at Ser-19 produces maximal force and additional phosphorylation at Thr-18 does not augment force development (23). In contrast to in vitro studies and smooth muscle contraction, in nonmuscle cells there is evidence of functional significance of diphosphorylation of myosin II. Studies examining activation of secretory processes in RBL-2H3 cells (8, 48) and platelets (34) suggest that diphosphorylation of myosin light chains correlates with cellular shape change and exocytosis. Likewise in HUVE, although the initial rise in tension is associated with monophosphorylation, development, and maintenance of tension correlates with sustained diphosphorylation. To identify the phosphorylation sites of myosin light chains in HUVE monolayers stimulated by thrombin, phosphopeptides were analyzed by one-dimensional isoelectric focusing (14, 54). Constitutive phosphorylation is catalyzed by MLCK in unstimulated cultures and consists of both mono- (Ser-19) and diphosphorylated (Ser-19/Thr-18) light chains. During thrombin stimulation, phosphorylation of myosin light chains is also catalyzed by MLCK with predominance of the diphosphopeptide, Ser-19/Thr-18. Throughout the time course of thrombin stimulation, no additional sites or switching of phosphorylation sites were detected as shown in antigen induced RBL-2H3 exocytosis (8, 48) or during the induction of cytokinesis (59, 76).

Moy et al. (53) investigating the effects of the inflammatory mediator histamine on HUVE myosin light chain phosphorylation, showed that histamine had a transient effect on light chain phosphorylation increasing phosphorylation by 0.18 mol PO_4/mol MLC that waned to baseline levels within 5 min. It is difficult to compare their studies with ours in view of the different agonists employed. It is also conceivable that these investigators have significantly underestimated the degree of light chain phosphorylation by not measuring the phosphorylated light chains in the 100,000-*g* pellet.

Having demonstrated that isometric tension development paralleled myosin light chain phosphorylation, we examined thrombin-induced HUVE cytoskeletal changes. We first investigated morphologically the time course and spatial rearrangements of F-actin and myosin II and then quantitated the cytoskeletal redistributions. Thrombin stimulation causes polymerization of actin that initially forms a fine network that progressively organizes into thick stress fibers that arrange parallel to one another. Myosin II changes from a diffuse amorphous pattern to organize in concert with actin filaments. The majority of soluble myosin II associates with the detergent insoluble cytoskeleton within 30 s. These data provide quantitative evidence that actin polymerization and myosin II filament formation occur simultaneously. Thrombin promotes the formation of individual fiber systems that interconnect to initiate and maintain isometric tension.

Actin polymerization regionally or globally within nonmuscle cells in response to soluble signals provides the polymer template necessary for cell shape change, cell motility and phagocytosis. Signal transduction induces functionally important actin structures that serve as an infrastructure for the interaction of cross-linking proteins necessary for cellular motile functions. The intent of this study was not to probe the mechanism of actin polymerization (review references 10, 36) however, these data raise questions that warrant further study: (*a*) does the energy produced from actin polymerization contribute to or generate isometric tension (10); (*b*) does actin polymerization occur solely from G-actin to F-actin or do various cellular actin pools contribute to the formation of the actin network (7, 68); (*c*) does cross-linking of the actin scaffold by actin binding proteins contribute to the maintenance of sustained tension (2, 25, 37, 62); and (*d*) is tension development a result of actin rearrangements or does tension dictate the reorganization of actin filaments?

Studies of the assembly properties of myosin II have consistently shown that myosin assembly and enzymatic activity are linked (27, 32). Our data from fluorescent images coupled with the myosin II association results implicates myosin II light chain phosphorylation as the critical event that initiates myosin II redistribution. Both morphological and quantitative data correlate temporally with the appearance of mono- and diphosphorylated light chains. It

seems plausible that monophosphorylation at Ser-19 initiates myosin binding to actin (2, 66). This would account for the dramatic drop in soluble myosin upon stimulation. As diphosphorylated myosin II comes to predominate, filaments polymerize and stabilize leading to the periodic distribution visualized fluorescently.

In conclusion, we propose that phosphorylation of myosin II light chains by MLCK is responsible for the thrombin induced increase in HUVE isometric tension. Monophosphorylation at Ser-19 precedes the development of tension while the rise and maintenance of sustained tension correlates with diphosphorylation at Ser-19/Thr-18. Since both activation/polymerization and reorganization of actin and myosin II occur concurrently, it is possible that the organizing actin network facilitates myosin II filament formation (2, 50) that in turn causes cross-linking and bundling of the actin network into actomyosin fibrils. The resulting rigid cross-linked actomyosin network would have an increased capacity to transduce agonist stimulated tension.

Regulation of contractility in nonmuscle cells has been assumed to be akin to the smooth muscle paradigm. Our studies from permeabilized endothelial cell preparations (73, 74) also suggested that this model was appropriate, however, data presented here demonstrates that whereas myosin light chain phosphorylation may be a common component of smooth muscle and HUVE monolayer contraction, the mechanism responsible for sustained tension in HUVE monolayers cannot be modeled in terms of the "latch state." Therefore we speculate that sustained isometric tension in HUVE monolayers results from maintenance of diphosphorylated (Ser-19/Thr-18) myosin light chains (phosphorylated latch bridges) and that reversal of diphosphorylation is associated with a decline in tension. In parallel, agonist activation promotes growth of a filamentous cytoskeleton that facilitates the function of myosin II as a tension-generating molecule. Modulation of this network with actin binding proteins (25, 37, 38, 62) could significantly amplify developed tension. Although these studies provide considerable evidence for the role of diphosphorylated myosin light chains in the development and maintenance of isometric tension in HUVE cells, further investigations are essential to more fully define the relationship between myosin light chain phosphorylation states and modulations in isometric tension.

We thank Dr. D. Lagunoff for helpful discussion and critical reading of the manuscript. We thank the Labor and Delivery staff at St. Johns Mercy Hospital, St. Louis, Missouri for their kind assistance.

This work was supported by National Institutes of Health grant HL-45788 to R. B. Wysolmerski. Shared Instrumentation grant RR-0566 was awarded to St. Louis University by the National Institutes of Health to establish a confocal imaging facility.

Received for publication 5 May 1995 and in revised form 10 May 1995.

References

1. Adelstein, R. S., and M. A. Conti. 1975. Phosphorylation of platelet myosin increases actin-activated myosin ATPase activity. *Nature (Lond.).* 256: 597–598.
2. Applegate, D., and J. D. Pardee. 1992. Actin-facilitated assembly of smooth muscle myosin induces formation of actomyosin fibrils. *J. Cell. Biol.* 117:1223–1230.
3. Barak, L. S., R. R. Yocum, E. A. Nothnogel, and W. W. Webb. 1980. Fluorescence staining of the actin cytoskeleton in living cells with 7-nitrobenz-2-nitrobenz-2-oxa-1, 3 diazole-phallacidin. *Proc. Natl. Acad. Sci. USA.* 77:980–984.
4. Borrione, A. C., A. M. C. Zanellato, L. Giuriato, G. Scannapieco, P. Pauletto, and S. Sartore. 1990. Nonmuscle and smooth muscle myosin isoforms in bovine endothelial cells. *Exp. Cell Res.* 190:1–10.
5. Bussolino, F., F. Silvagno, G. Garbarino, C. Costamagna, F. Sanavio, M. Arese, R. Soldi, M. Aglietta, G. Pescarmona, G. Camussi, and A. Bosia. 1994. Human endothelial cells are targets for platelet-activating factor (PAF) activation of α and β protein kinase C isozymes in endothelial cells stimulated by PAF. *J. Biol. Chem.* 269:2877–2886.
6. Cande, W. Z., and R. M. Ezzell. 1986. Evidence for regulation of lamellipodial and tail contraction of glycerinated chicken embryonic fibroblasts by myosin light chain kinase. *Cell Motil. Cytoskeleton.* 6:640–648.
7. Cassimeris, L., H. McNeill, and S. H. Zigmond. 1990. Chemoattractant-stimulated polymorphonuclear leukocytes contain two populations of actin filaments that differ in their spatial distributions and relative stabilities. *J. Cell Biol.* 110:1067–1075.
8. Choi, O. H., R. S. Adelstein, and M. A. Beaven. 1994. Secretion from rat basophilic RBL-2H3 cells is associated with diphosphorylation of myosin light chains by myosin light chain kinase as well as phosphorylation by protein kinase C. *J. Biol. Chem.* 269:536–541.
9. Colburn, J. C., C. H. Michnoff, L. C. Hsu, C. A. Slaughter, K. E. Kamm, and J. T. Stull. 1988. Sites phosphorylated in myson light chain in contracting smooth muscle. *J. Biol. Chem.* 263:19166–19173.
10. Cooper, J. A. 1991. The role of actin polymerization in cell motility. *Annu. Rev. Physiol.* 53:585–605.
11. Corson, M. A., J. R. Sellers, R. S. Adelstein, and M. Schoenberg. 1990. Substance P contracts bovine tracheal smooth muscle via activation of myosin light chain kinase. *Am. J. Physiol.* 259:C258–C265.
12. Craig, R., R. Smith, and J. Kendrick-Jones. 1983. Light-chain phosphorylation controls the conformation of vertebrate non-muscle and smooth muscle myosin molecules. *Nature (Lond.).* 302:436–439.
13. Cross, R. A., A. P. Jackson, S. Citi, J. Kendrick-Jones, and C. R. Bagshaw. 1988. Active site trapping of nucleotide by smooth and non-muscle myosins. *J. Mol. Biol.* 203:173–181.
14. Daniel, J. L., and J. R. Sellers. 1992. Purification and characterization of platelet myosin. *Methods Enzymol.* 215:78–88.
15. Dillon, P. F., M. O. Aksoy, S. P. Driska, and R. A. Murphy. 1981. Myosin phosphorylation and the cross-bridge cycle in arterial smooth muscle. *Science (Wash. DC).* 211:495–497.
16. Erdodi, F., M. Barany, and K. Barany. 1987. Myosin light chain isoforms and their phosphorylation in arterial smooth muscle. *Circ. Res.* 61:898–903.
17. Fechheimer, M., and J. J. Cebra. 1982. Phosphorylation of lymphocyte myosin catalyzed in vitro and in intact cells. *J. Cell Biol.* 93:261–268.
18. Gelsema, W. J., C. L. DeLigny, and N. G. Van Der Veen. 1979. Isoelectric points of proteins determined by isoelectric focusing in the presence of urea and ethanol. *J. Chrom.* 171:171–181.
19. Gerthoffer, W. T. 1991. Regulation of the contractile element of airway smooth muscle. *Am. J. Physiol.* 261:L15–L28.
20. Giloh, H., and J. W. Sedat. 1982. Fluorescence microscopy: reduced photobleaching of rhodamine and fluorescein conjugates by *n*-propyl gallate. *Science (Wash. DC).* 217:1252–1255.
21. Grant, J. W., M. B. Taubman, S. L. Church, R. L. Johnson, and B. Nadal-Ginard. 1990. Mammalian nonsarcomeric myosin regulatory light chains are encoded by two differentially regulated linked genes. *J. Cell Biol.* 111: 1127–1135.
22. Greenberg, S., J. El Khoury, F. DiVirgilio, E. M. Kaplan, and S. C. Silverstein. 1991. Ca^{2+}-independent f-actin assembly and dissembly during fc receptor-mediated phagocytosis in mouse macrophages. *J. Cell Biol.* 113: 757–767.
23. Haeberle, J. R., T. A. Sutton, and B. A. Trockman. 1988. Phosphorylation of two sites on smooth myosin effects on contraction of glycerinated vascular smooth muscle. *J. Biol. Chem.* 263:4424–4429.
24. Hai, C.-M., and R. A. Murphy. 1989. Ca^{2+}, crossbridge phosphorylation, and contraction. *Annu. Rev. Physiol.* 51:285–298.
25. Hayakawa, K., T. Okagaki, S. Higashi-Fujime, and K. Kohama. 1994. Bundling of actin filaments by myosin light chain kinase from smooth muscle. *Biochem. Biophys. Res. Commun.* 199:786–791.
26. He, Y., and F. Grinnell. 1994. Stress relaxation of fibroblasts activates a cyclic AMP signaling pathway. *J. Cell Biol.* 126:457–464.
27. Higashihara, M., D. J. Hartshorne, R. Craig, and M. Ikebe. 1989. Correlation of enzymatic properties and conformation of bovine erythrocyte myosin. *Biochemistry.* 28:1642–1649.
28. Hochstrasser, D. F., M. G. Harrington, A. C. Hochstrasser, M. J. Miller, and C. R. Merril. 1988. Methods for increasing the resolution of two-dimensional protein electrophoresis. *Anal. Biochem.* 173:424–435.
29. Holzapfel, G., J. Wehland, and K. Weber. 1983. Calcium control of actin-myosin based contraction in triton models of 3T3 fibroblasts is mediated by the myosin light chain kinase (MLCK)-calmodulin complex. *Exp. Cell Res.* 148:117–126.
30. Horgan, M. J., J. W. Fenton II, and A. B. Malik. 1987. Alpha-thrombin-induced pulmonary vasoconstriction. *J. Appl. Physiol.* 63: 1993–2000.
31. Ikebe, M., and D. J. Hartshorne. 1985. Phosphorylation of smooth muscle myosin at two distinct sites by myosin light kinase. *J. Biol. Chem.* 260:

10027–10031.
32. Ikebe, M., J. Koretz, and D. J. Hartshorne. 1988. Effects of phosphorylation of light chain residues threonine 18 and serine 19 on the properties and conformation of smooth muscle myosin. *J. Biol. Chem.* 263:6432–6437.
33. Ikebe, I., D. J. Hartshorne, and M. Elzinga. 1986. Identification, phosphorylation, and dephosphorylation of a second site for myosin light chain kinase on the 20,000-dalton light chain of smooth muscle myosin. *J. Biol. Chem.* 261:36–39.
34. Itoh, K., T. Hara, F. Yamada, and N. Shibata. 1992. Diphosphorylation of platelet myosin ex vivo in the initial phase of activation by thrombin. *Biochim. Biophys. Acta.* 1136:52–56.
35. Jaffe, E. A., R. L. Nachman, C. G. Becker, and C. R. Minick. 1973. Culture of human endothelial cells derived from umbilical veins: identification by morphological and immunological criteria. *J. Clin. Invest.* 52:2745–2756.
36. Janmey, P. A. 1994. Phosphoinositides and calcium as regulators of cellular actin assembly and disassembly. *Annu. Rev. Physiol.* 56:169–191.
37. Janson, L. W., J. R. Sellers, and D. L. Taylor. 1992. Actin-binding proteins regulate the work performed by myosin II on single actin filaments. *Cell Motil. Cytoskeleton.* 22:274–280.
38. Kanoh, S., M. Ito, E. Niwa, Y. Kawano, and D. J. Hartshorne. 1993. Actin-binding peptide from smooth muscle myosin light chain kinase. *Biochemistry.* 32:8902–8907.
39. Kawamoto, S., and R. S. Adelstein. 1988. The heavy chain of smooth muscle is phosphorylated in aorta cells. *J. Biol. Chem.* 263:1099–1102.
40. Kawamoto, S., A. R. Bengur, J. R. Sellers, and R. S. Adelstein. 1989. In situ phosphorylation of human platelet myosin heavy and light chains by protein kinase C. *J. Biol. Chem.* 264:2258–2265.
41. Kolodney, M. S., and R. B. Wysolmerski. 1992. Isometric contraction by fibroblasts and endothelial cells in tissue culture: a quantitative study. *J. Cell Biol.* 117:73–82.
42. Kolodney, M. S., and E. L. Elson. 1993. Correlation of myosin light chain phosphorylation with isometric contraction of fibroblasts. *J. Biol. Chem.* 268:23850–23855.
43. Kumar, C. C., S. R. Mohan, P. J. Zavodny, S. K. Narula, and P. J. Leibowitz. 1989. Characterization and differential expression of human vascular smooth muscle myosin light chain 2 isoform in nonmuscle cells. *Biochemistry.* 28:4027–4035.
44. Laemmli, U. K. 1970. Cleavage of structural proteins during the assembly of the head of bacteriophage T4. *Nature (Lond.).* 227:680–685.
45. Lagunoff, D., and A. Rickard. 1987. Methods for the study of rat peritoneal mast cell secretion. *In* In Vitro methods for Studying Secretion. A. M. Poisner and J. M. Trefaro, editors. Elsevier, Amersterdam, Netherlands. 13–28.
46. Lansman, J. B., T. J. Hallam, and T. J. Rink. 1987. Single stretch-activated ion channels in vascular endothelial cells as mechanotransducers? *Nature (Lond.).* 325:811–813.
47. Laposata, M., D. K. Dovnarsky, and H. S. Shin. 1982. Thrombin-induced gap formation in confluent endothelial cell monolayers in vitro. *Blood.* 62:549–556.
48. Ludowyke, R. I., I. Peleg, M. A. Beaven, and R. S. Adelstein. 1989. Antigen-induced secretion of histamine and the phosphorylation of myosin by protein kinase C in rat basophilic leukemia cells. *J. Biol. Chem.* 264: 12492–12501.
49. Lundell, M. J., and J. Hirsh. 1994. A new visible light DNA fluorochrome for confocal microscopy. *Biotechniques.* 16:434–440.
50. Mahajan, R. K., K. T. Vaughan, J. A. Johns, and J. D. Pardee. 1989. Actin filaments mediate dictyostelium myosin assembly in vitro. *Proc. Natl. Acad. Sci. USA.* 86:6161–6165.
51. Majno, G., and G. E. Palade. 1961. Studies on inflammation I. The effect of histamine and serotonin on vascular permeability: an electron microscopic study. *J. Biophys. Biochem. Cytol.* 11:571–585.
52. Miller-Hance, W. C., J. R. Miller, J. N. Wells, J. T. Stull, and K. E. Kamm. 1988. Biochemical events associated with activation of smooth muscle contraction. *J. Biol. Chem.* 263:13979–13982.
53. Moy, A. B., S. S. Shasby, B. D. Scott, and D. M. Shasby. 1993. The effect of histamine and cyclic adenosine monophosphate on myosin light chain phosphorylation in human umbilical vein endothelial cells. *J. Clin. Invest.* 92:1198–1206.
54. Nakabayashi, H., J. R. Sellers., and K. P. Huang. 1991. Catalytic fragment of protein kinase C exhibits altered substrate specificity toward smooth muscle myosin light chain. *FEBS Lett.* 294:144–148.
55. O'Farrel, P. H. 1975. High resolution two-dimensional electrophoresis of proteins. *J. Biol. Chem.* 250:4007–4021.
56. Pender, N., and C. A. G. McCulloch. 1991. Quantitation of actin polymerization in two human fibroblast sub-types responding to mechanical stretching. *J. Cell. Sci.* 100:189–193.
57. Rembold, C. M., and R. A. Murphy. 1993. Models of the mechanism for crossbridge attachment in smooth muscle. *J. Muscle Res. Cell Motil.* 14: 325–333.
58. Rotrosen, D. J., and J. I. Gallin. 1986. Histamine type I receptors occupancy increases endothelial cell cytosolic calcium, reduces f-actin, and promotes albumin diffusion across cultured endothelial monolayers. *J. Cell Biol.* 103:2379–2387.
59. Satterwhite, L. L., M. J. Lohka, K. L. Wilson, T. Y. Scherson, L. J. Cisek, J. L. Corden, and T. D.. Pollard. 1992. Phosphorylation of myosin-II regulatory light chain by cyclin-p34^{cdc2} a mechanism for the timing of cytokinesis. *J. Cell Biol.* 118:595–605.
60. Schnittler, H.-J., A. Wilke, T. Gress, N. Suttorp, and D. Drenckhahn. 1990. Role of actin and myosin in the control of paracellular permeability in pig, rat and human vascular endothelium. *J. Physiol.* 431:379–401.
61. Shuman, M. R., and P. W. Majerus. 1976. The measurement of thrombin in clotting blood by radioimmunoassay. *J. Clin. Invest.* 58:1249–1258.
62. Stossel, T. P. 1982. The structure of cortical cytoplasm. *Phil. Trans. R. Soc. Lond. B.* 299:275–289.
63. Sumpio, B. E., A. J. Banes, M. Buckley, and G. Johnson. 1988. Alterations in aortic endothelial cell morphology and cytoskeleton protein synthesis during cyclic tensional deformation. *J. Vasc. Surg.* 7:130–138.
64. Taubman, M. B., J. W. Grant, and B. Nadal-Ginard. 1987. Cloning and characterization of mammalian myosin regulatory light chain (rlc) cDNA: the rlc gene is expressed in smooth, sarcomeric, and nonmuscle tissue. *J. Cell Biol.* 104:1505–1513.
65. Trotter, J. A., S. P. Scordilis, and S. S. Margossian. 1983. Macrophages contain at least two myosins. *FEBS Lett.* 156:135–140.
66. Trybus, K. M., and S. Lowey. 1985. Mechanism of smooth muscle myosin phosphorylation. *J Biol. Chem.* 260:15988–15995.
67. Umemoto, S., R. Bengur, and J. R. Sellers. 1989. Effect of multiple phosphorylations of smooth muscle and cytoplasmic myosins on movement in an in vitro motility assay. *J. Biol. Chem.* 264:1431–1436.
68. Watts, R. G., and T. H. Howard. 1992. Evidence for a gelsolin-rich, labile f-actin pool in human polymorphonuclear leukocytes. *Cell Motil. Cytoskeleton.* 21:25–37.
69. West, D. C., A. Sattar, and S. Kumar. 1985. A simplified in situ solubilization procedure for the determination of DNA and cell number in tissue cultured mammalian cells. *Anal. Biochem.* 147:289–295.
70. Wirz, H. W., and L. G. Dobbs. 1990. Calcium mobilization and exocytosis after one mechanical stretch of lung epithelial cells. *Science (Wash. DC).* 250:1266–1269.
71. Wysolmerski, R., and D. Lagunoff. 1985. The effect of ethchlorvynol on cultured endothelial cells. A model for the study of the mechanism of increased vascular permeability. *Am. J. Pathol.* 119:505–512.
72. Wysolmerski, R. B., and D. Lagunoff. 1988. Inhibition of endothelial cell retraction by ATP depletion. *Am J. Path.* 132:28–37.
73. Wysolmerski, R. B., and D. Lagunoff. 1990. Involvement of myosin light-chain kinase in endothelial cell retraction. *Proc. Natl. Acad. Sci. USA.* 87: 16–20.
74. Wysolmerski, R. B., and D. Lagunoff. 1991. Regulation of permeabilized endothelial cell retraction by myosin phosphorylation. *Am. J. Physiol.* 30: C32–C40.
75. Wysolmerski, R. B., D. Lagunoff, and T. Dahms. 1984. Ethchlorvynol-induced pulmonary edema in rats: an ultrastructural study. *Am. J. Pathol.* 115:447–457.
76. Yamakita, Y., S. Yamashiro, and F. Matsumura. 1994. In vivo phosphorylation of regulatory light chain of myosin II during mitosis of cultured cells. *J. Cell Biol.* 124:129–137.